

Spin Period Evolution of Recycled Pulsar in Accreting Binary

J. Wang¹, C.M. Zhang¹, Y.H. Zhao¹, Y. Kojima², H. X. Yin³, and L.M. Song⁴

¹ National Astronomical Observatories, Chinese Academy of Sciences, Beijing 100012, China,
e-mail: zhangcm@bao.ac.cn

² Department of Physics, Hiroshima University, Higashi-Hiroshima 739-8526, Japan

³ School of Space Science and Physics, Shandong University, Weihai 264209, China

⁴ Institute of High Energy Physics, Chinese Academy of Sciences, Beijing 100049, P. R. China

the date of receipt and acceptance should be inserted later

Abstract. We investigate the spin-period evolutions of recycled pulsars in binary accreting systems. Taking both the accretion induced field decay and spin-up into consideration, we calculate their spin-period evolutions influenced by the initial magnetic-field strengths, initial spin-periods and accretion rates, respectively. The results indicate that the minimum spin-period (or maximum spin frequency) of millisecond pulsar (MSP) is independent of the initial conditions and accretion rate when the neutron star (NS) accretes $\sim 0.2M_{\odot}$. The accretion torque with the fastness parameter and gravitational wave (GW) radiation torque may be responsible for the formation of the minimum spin-period (maximum spin frequency). The fastest spin frequency (716 Hz) of MSP can be inferred to associate with a critical fastness parameter about $\omega_c = 0.55$. Furthermore, the comparisons with the observational data are presented in the field-period ($B - P$) diagram.

Key words. accretion: accretion disks—stars:neutron— binaries: close—X-rays: stars—pulsar

1. Introduction

Neutron stars (NSs) are usually detected as either normal pulsars (single or in a binary) with magnetic-field $B \sim 10^{12}$ G and spin-period $P \sim 0.5$ s, or millisecond pulsars (MSPs) (half in binary) with $B \sim 10^{8.5}$ G and $P \sim 20$ ms (e.g. Bhattacharya & van den Heuvel 1991; Lorimer 2008). The spin-periods and surface magnetic-fields assigned to these two different systems are found to span different ranges of $B - P$ values (Hobbs & Manchester 2004; Manchester et al. 2005; Lorimer 2008), and the updated statistical distributions of B and P are plotted in Fig. 1 (data from ATNF pulsar catalogue). In this figure, we notice that the distributions of both B and P are almost bimodal, as firstly suggested by Camilo et al. (1994), with a dichotomy between "normal" pulsars ($P \sim 0.1$ s - 10 s and $B \sim 10^{11}$ G - 10^{13} G) and MSPs ($P \sim 1$ ms - 20 ms and $B \sim 10^8$ G - 10^9 G). This abnormal phenomenon has led to the idea that radio pulsars in binary systems have been "recycled", i.e. they have been spun up due to mass accretion during the phase of mass exchange in binaries (Alpar et al. 1982; Radhakrishnan & Srinivasan 1982; Bhattacharya & Srinivasan 1995). The weak magnetic-field of MSP strongly supports the idea that it decays in the binary accretion phase (e.g. Taam & van den Heuvel 1986; van den Heuvel 2004). The currently widely accepted view about this phenomenon is the accretion-induced evolution, i.e., NSs accreting materials from their low-mass binary

companions are spun up by the angular momentum carried by the accreted materials, while the magnetic-field decays (Taam & van den Heuvel 1986; Bhattacharya & van den Heuvel 1991; van den Heuvel 2004). The X-ray binaries are the evolutionary precursors to these "recycled" MSPs. It is evident that B and P of X-Ray pulsars and recycled pulsars are correlated with the duration of both the accretion phase and the total amount of matter accreted (Taam & van den Heuvel 1986; Shibazaki et al. 1989). If the NS accretes a small quantity of mass from its companion, e.g. $\sim 0.001M_{\odot} - 0.01M_{\odot}$, a recycled pulsar with the mildly weak field and short spin-period ($B \sim 10^{10}$ G, $P \sim 50$ ms) will be formed (e.g. Francischelli, Wijers & Brown 2002), like PSR 1913+16 and PSR J0737-3039 (Lyne et al. 2004). The direct evidence for this recycled idea has been found in low mass X-ray binary (LMXB) with the accretion millisecond X-ray pulsar (AMXP), e.g. Sax J 1808.4-3658 (Wijnands & Klis 1998), and in observing the transition link from an X-ray binary to a radio pulsar PSR J1023+0038 (Archibald et al. 2009).

At the end of the accretion phase of NS/LMXB (accreted mass $\sim 0.2M_{\odot}$), the NS magnetic-field may arrive at a bottom value about 10^8 G and spin-period may reach a minimum about millisecond (Cheng & Zhang 1998, 2000), remaining a MSP (van den Heuvel & Bitzaraki 1995ab). Since then, spin-down due to dipole radiation has been conceived as the "standard evolution" of MSP (Urpin & Konenkov 1997; Urpin, Geppert &

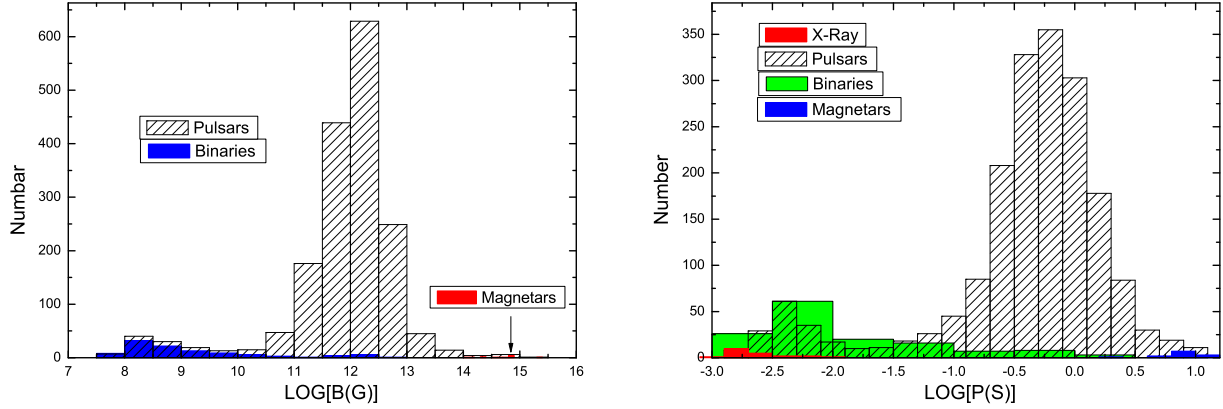


Fig. 1. Distribution of magnetic-field and spin-period for 1864 pulsars (data from the ATNF pulsar catalogue, see Manchester et al. 2005). Here, 141 binary pulsars and 13 magnetars (Kouveliotou 2003) are separately identified for the statistics of magnetic-field and spin-period. The 24 accretion millisecond X-ray pulsars discovered by RXTE (see e.g. Wijnands 2005; Lamb & Yu 2005; Yin et al. 2007) are put in the spin-period histogram.

Konenkov 1997, 1998). The switch-on of a radio pulsar could exist, whose radiation pressure is capable of ejecting the accreted matter out of the system and prevent any further accretion. This 'radio ejection' phase in the binary will account for the formation of a MSP (Burderi et al. 2002ab). However, the question whether all observed MSPs could be produced within this recycled framework has not been quantitatively addressed until now. The accretion induced collapse (AIC) of a white dwarf as an alternative mechanism for the formation of MSP has been studied recently (Ferrario & Wickramasinghe 2007ab; Hurley et al. 2009; Wickramasinghe et al. 2009). Recently, another idea for MSP formation is proposed, which claims that these objects are born with low magnetic fields (Halpern & Gotthelf 2010).

Then the mechanisms for the accretion-driven field decay and spin-up in binary NSs have been suggested by many researchers in various proposals. The accretion flow and thermal effects speed-up Ohmic dissipation of NS crust currents, which accounts for the field decay and spin evolution (Geppert & Urpin 1994; Geppert, Page & Zannias 1999; Urpin & Geppert 1995; Romani 1990). The interactions between the accreted matter and magnetic-field in the course of accretion phase are studied to account for the field decay (Melatos & Phinney 2001; Payne & Melatos 2004; Konar & Bhattacharya 1999; Konar & Choudhury 2004; Lovelace, Romanova & Bisnovaty-Kogan 2005). Not only is the total amount of accreted mass considered to influence the final field strength and minimum spin-period (van den Heuvel 1995; van den Heuvel & Bitzaraki 1994, 1995ab), but also the influences of accretion rate may be a factor (Wijers 1997; Cumming et al. 2001; Cumming 2005; Zhang & Kojima 2006).

Taking the accretion-induced field decay into consideration, we investigate the formation of the high spin frequency (short spin-period) for a MSP, and the influences on it by the initial conditions (e.g. initial spin-period and initial field) and accretion rate. The spin-up torque and field evolution make their spin-period and field distributions in $B - P$ diagram to

change from the regions of $B \sim 10^{11-13}$ G and $P \sim 1$ s - 100 s to that of $B \sim 10^{8-9}$ G and $P \sim 1$ ms - 20 ms as observed. This paper is organized as follows. In Section 2, we review the main equations that dominate the $B - P$ relation in the accretion phase. The effects by the initial conditions and accretion rate on the spin-period are presented in Section 3. Section 4 contains the summary and discussion.

2. Field Versus Period Relation

2.1. Description for the Model

As declaimed by the accretion induced magnetic field decay model (Zhang & Kojima 2006), if the magnetic field is sufficiently strong, e.g. $\sim 10^{12}$ G, and the star spin very slowly initially, the accreted matter will be channeled onto the polar patches by the field lines, where the compressed accreted matter causes the expansion of magnetic polar zone in two directions, downward and equatorward, which makes the magnetic flux in the polar zone diluted. With accretion, the field decays and magnetosphere shrinks until the magnetosphere reaches the surface of NS, where a bottom field is obtained to be about $\sim 10^8$ G.

Based on the above model, the accretion-induced field evolution is obtained analytically with the initial field $B(t = 0) = B_0$ (Zhang & Kojima 2006),

$$B = \frac{B_f}{(1 - [C \exp(-y) - 1]^2)^{1/4}}. \quad (1)$$

Here, we define the parameters as follows, $y = \frac{2\Delta M}{7M_{cr}}$, the accreted mass $\Delta M = \dot{M}t$, the crust mass $M_{cr} \sim 0.2M_\odot$, $C = 1 + \sqrt{1 - x_0^2} \sim 2$ with $x_0^2 = (\frac{B_f}{B_0})^{4/7}$. B_f is the bottom magnetic-field which is defined by the NS magnetosphere radius matching the stellar radius, i.e., $R_M(B_f) = R$. R_M is defined as $R_M = \phi R_A$ where *Alfvén* radius R_A (Elsner & Lamb 1977;

Ghosh & Lamb 1977) reads,

$$R_A = 3.2 \times 10^8 (\text{cm}) \dot{M}_{17}^{-2/7} \mu_{30}^{4/7} m^{-1/7}, \quad (2)$$

The model dependent parameter ϕ is about 0.5 (Ghosh & Lamb 1979b hereafter GL; Shapiro & Teukolsky 1983; Frank et al. 2002). \dot{M}_{17} is the accretion rate in units of 10^{17} g/s. μ_{30} is the magnetic moment in units of 10^{30} Gcm³. The mass $m = M/M_\odot$ is in the unit of solar mass. Using the relation $R_M(B_f) = R$, we can obtain the bottom field,

$$B_f = 1.32 \times 10^8 (\text{G}) \left(\frac{\dot{M}}{\dot{M}_{18}} \right)^{1/2} m^{1/4} R_6^{-5/4} \phi^{-7/4}, \quad (3)$$

where $\dot{M}_{18} = \dot{M}/10^{18}$ g/s and $R_6 = R/10^6$ cm. As declaimed by Inogamov & Sunyaev (1999), in the accretion process, a boundary layer forms between the innermost disk and magnetosphere due to the transition for rotating velocity of plasma from Keplerian to the spin velocity of NS. When the accretion rate increases, this layer may spread (Inogamov & Sunyaev 1999), and as a result more matter is accreted to the polar gap and diffuses to the entire surface of the NS. **This effect will influence on the field decay efficiency of the model by Zhang & Kojima (2004), since some spreading matter has little contribution to the field lines dragging of the polar patches. Moreover, such a spreading will expand the polar cap area, which makes the polar cap to occupy the entire NS surface while the magnetosphere does not reach the NS radius. The bottom field of NS is determined by the condition that the magnetosphere equals the NS radius (Zhang & Kojima 2004). If there is no field decay while the magnetosphere radius is bigger than NS radius, then the modified bottom field by considering the spreading of the polar cap will be bigger than the one obtained for the ideal frozen plasma in polar cap zone. Namely, the magnetic field of recycled NS is slight bigger than the ideal value of the model by Zhang & Kojima (2004).**

To study the spin evolution of NS in accretion phase, we employ the formula for accretion-induced spin-up given by GL,

$$-\dot{P} = 5.8 \times 10^{-5} \left[\left(\frac{M}{M_\odot} \right)^{-3/7} R_6^{12/7} I_{45}^{-1} \right] \times B_{12}^{7/2} (PL_{37}^{3/2})^2 n(\omega_s) \text{ syr}^{-1}, \quad (4)$$

where we define the parameters, the surface field $B_{12} = B/10^{12}$ G, the moment of inertia $I_{45} = I/10^{45}$ gcm², the X-ray brightness ($L = GMM/R$) L_{37} in units of 10^{37} erg/s, respectively. The dimensionless parameter $n(\omega_s)$ is the fastness parameter which is explained in the following subsection.

2.2. Fastness Parameter

For a slowly rotating magnetic NS, the rotation of the star couples to the orbital motion of the disk matter at the Alfvén radius when accretion flow is approximately radial. So the limit of angular velocity ($\Omega_s = 2\pi/P$) for a NS can reach the Keplerian velocity ($\Omega_k(R_M) = \sqrt{GM/R_M^3}$). In general, the spin velocity is always less than the orbital velocity, i.e. $\Omega_s \ll \Omega_k(R_M) = \sqrt{GM/R_M^3}$. Therefore, the relative importance of stellar rotation

can be described by the ratio parameter of the angular velocities (Elsner & Lamb 1977; Ghosh & Lamb 1977; Li & Wang 1996, 1999; Shapiro & Teukolsky 1983),

$$\omega_s \equiv \frac{\Omega_s}{\Omega_k(R_M)} = 1.35 \left[\left(\frac{M}{M_\odot} \right)^{-2/7} R_6^{15/7} \right] B_{12}^{6/7} P^{-1} L_{37}^{-3/7}, \quad (5)$$

which plays a significant role in our entire understanding of accretion to the rotating magnetic NSs.

To calculate the accretion torque which acts on a magnetic NS accreting matter from a disk, GL introduced a dimensionless accretion torque $n(\omega_s)$ depending primarily on the fastness parameter. A simple expression for $n(\omega_s)$ is given by GL,

$$n(\omega_s) = 1.4 \times \left(\frac{1 - \omega_s/\omega_c}{1 - \omega_s} \right), \quad (6)$$

where ω_c is the critical value. For a slowly rotating star ($\omega_s \ll 1$), GL found that the dimensionless function $n(\omega_s)$ decreases with ω_s and become negative for $\omega_s > \omega_c$ if $n(\omega_s) \sim 1.4$. In addition, GL also stressed $\omega_c \sim 0.35$ for their model. However, the subsequent work (Ghosh & Lamb 1992) indicates that ω_c is unlikely to be less than 0.2, but it could be as large as 0.9. By the aid of this dimensionless parameter, we can establish the relation between the total torque on the star and the torque communicated to the star by the magnetic-field lines that thread the inner transition zone.

In the following subsections, we study the spin evolution of NS in a binary system, where the influence by fastness is included.

3. Spin Evolution of Accreting NS

In this section, we investigate the spin-period evolution of accreting NSs by solving equations (1), (4), (5) and (6) with different initial conditions and accretion rates, where we set the usual parameters for NS, e.g. $m = 1.4$, $R_6 = 1.5$, $\phi = 0.5$ and $M_{\text{cr}} = 0.2M_\odot$.

3.1. Influence by Initial Conditions

We consider the spin evolution for a wide range of initial conditions (initial magnetic-fields and initial spin-periods): (1). varying the initial magnetic-field 5×10^{11} G, 5×10^{12} G and 5×10^{13} G while setting spin-period and accretion rate as 100 s and \dot{M}_{17} , respectively (Fig. 2); (2). varying the initial spin-period 1 s, 10 s & 100 s with a certain field (5×10^{12} G) and constant accretion rate (\dot{M}_{17}) (Fig. 3).

For the samples, we classify them as normal pulsars, MSPs and binaries. From the figures, we can see that most MSPs are consistent with the binary pulsars, while only a few binaries fall in the same region of the normal pulsars that have a magnetic-field $\sim > 10^{11}$ G. Recycled pulsars are expected to be found only to the right of the spin-up line and to the left of the "death-line" (Bhattacharya & van den Heuvel 1991), which is shown indeed the case in these figures (Fig. 2, Fig. 3) for almost all the binaries and MSPs. This strongly supports the view that the MSPs have been recycled (Alpar et al. 1982; Radhakrishnan & Srinivasan 1982). Firstly, with a small amount of mass transferred, the NS is spun-up from the death valley with long period

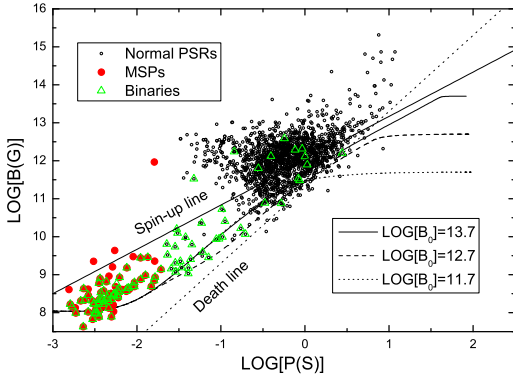


Fig. 2. The diagram of the magnetic-field versus spin-period for pulsars. The spin-up line represents the minimum spin-period to which such a spin-up may proceed in an Eddington-limited accretion, while the “death-line” corresponds to a polar cap voltage below which the pulsar activity is likely to switch off (Bhattacharya & van den Heuvel 1991). The evolutionary tracks in $B-P$ diagram are plotted with different initial magnetic-field strengths, but with same initial spin-period ($P_o = 100$ s) and same accretion rate \dot{M}_{17} ; The solid, dash and dot lines denote the numerical solutions for equations (1), (4), (5) and (6) with initial field $B_o = 5 \times 10^{13}$ G, 5×10^{12} G and 5×10^{11} G, respectively.

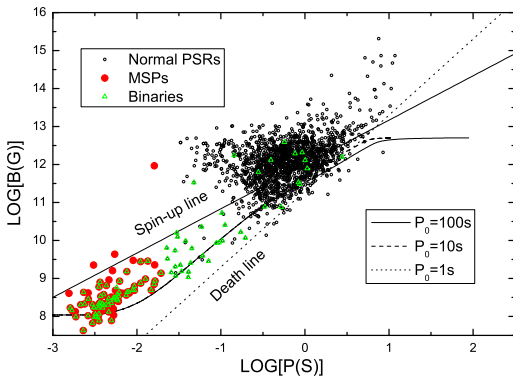


Fig. 3. The same meaning as Fig. 2 with different initial spin-periods ($P_o = 1$ s - dot line, 10 s - dash line, 100 s - solid line) at the fixed initial magnetic-field ($B_o = 5 \times 10^{12}$ G) and same accretion rate \dot{M}_{17} .

and strong field, e.g. the NS in HMXBs ($B \sim 10^{12}$ G, $P \sim 10$ s) like Her X-1 ($P = 1.24$ s, $B = 3 \times 10^{12}$ G, see van der Meer et al. 2007). With the long-lived accretion phase the binary accepts sufficient mass from its companion and the NS yield a substantial field decay, as in the case of MSPs (Bhattacharya & van den Heuvel 1991), e.g., the fastest known pulsar PSR J1748-2446 ($B \sim 10^8$ G, $P = 1.4$ ms, see Hessels et al. 2006).

As shown in Fig.2, three B-P tracks with the different initial field values begin to follow one track when the spin period

evolves to the hundred millisecond regime, and here the system accretes $\sim 0.01 M_\odot$. After the system accretes about $\sim 0.2 M_\odot$, the field reaches $\sim 10^8$ G – a bottom value, and the spin period enters the millisecond regime, which is inferred corresponding to the condition $\omega_s = \omega_c$. Namely, the bottom spin period or maximum spin frequency can be obtained by

$$v_{sMax} = v_k(R_M = R)\omega_c, \quad (7)$$

where $v_k(R_M = R) = 1300(\text{Hz})(M/1.4M_\odot)^{1/2}(R/15\text{km})^{-3/2}$ is the maximum spin frequency at stellar surface. If the critical fastness parameter is $\omega_c = 0.55$, then the maximum spin frequency can be as high as 715 Hz, which is similar to the fastest spin frequency of MSP observed (716 Hz). The lower the critical fastness, the lower the final spin frequency achieved.

For our numerical calculation, we take the effect of fastness parameter into consideration. If the critical fastness parameter is set as 0.9, the numerical solutions for equations (1), (4), (5) and (6) suggest that the evolutionary curves in the $B-P$ diagram are a little below the spin-period equilibrium line. However, the effect of the fastness parameter is significant when the B-P evolutionary track is close to the equilibrium period line (spin-up line). This indicates that the spin angular velocity of the star tends to reach the Keplerian angular velocity at the inner edge of the accretion disk, but never exceeds this angular velocity. In fact, the primary effect of the fastness parameter is to force the evolution curves back to or below the equilibrium period line and ensure that the evolutionary track cannot go beyond this line.

From these tracks, we can see that despite of the differences for initial fields and initial spin periods, the NSs can approach at a certain minimum spin period and bottom field after accreting $\sim 0.2 M_\odot$. If the accreting phase is over, a recycled pulsar can be found in the region of $B-P$ diagram with $B \sim 10^{8-9}$ G and $P \sim 10$ ms, forming a MSP. On account of the existence of minimum spin-period and bottom field (e. g. $B \sim 10^8$ G), the P-distribution and B-distribution imply that the MSPs accumulate close to the region of low field and short period, which is an explanation of the bimodal distributions for all pulsars, as shown in Fig.1. In short, for LMXBs the different initials give the similar final value of spin-period, which is insensitive to the initial conditions.

3.2. Influence by Accretion Rate

In this part, we study the influence by accretion rates on the spin-period evolution. We set the accretion rate as \dot{M}_{16} , \dot{M}_{17} and \dot{M}_{18} at the fixed magnetic-field (5×10^{12} G) and spin-period (100 s), respectively (see Fig. 4). From the Fig. 4, we find that, with different accretion rate, the spin evolution follows different tracks. If we set the critical fastness parameter as 0.9, the tracks with Eddington accretion rate ($\dot{M}_{18} = 1$) matches the evolution of most recycled pulsars well, but the track with \dot{M}_{16} lies below the “death-line”. Moreover, the curves with a high accretion rate and high critical fastness have the tendency to approach the spin-up line.

For a comparison of the magnetic-field and spin-period distributions between theory and observation, we plot the statistical distributions of magnetic-field and spin-period

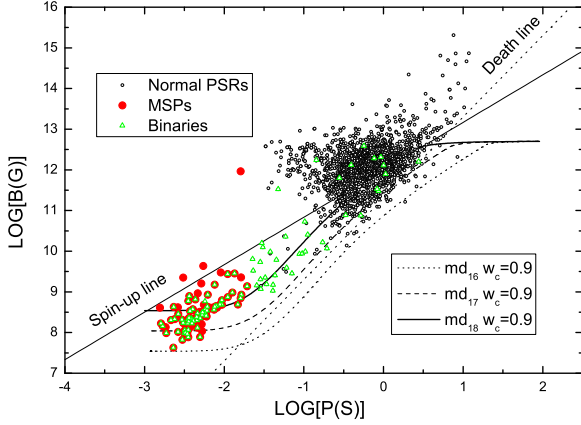


Fig. 4. The same meaning as Fig. 2 with different accretion rates, at the fixed initial magnetic-field ($B_o = 5 \times 10^{12} G$) and initial spin-period ($P_o = 100s$), from the upper to bottom, \dot{M}_{18} - solid line, \dot{M}_{17} - Dash line and \dot{M}_{16} - dot line, corresponding to the bottom fields of $\sim 10^{7.5} G$, $\sim 10^8 G$ and $\sim 10^{8.5} G$, respectively. The critical fastness parameter is set to be $\omega_c = 0.9$.

obtained from the calculation for theoretical model with various initial conditions (see caption of Fig. 5). 100 samples of final B-field and final spin period (B, P) have been done, which are plotted to compare the observed data of binary pulsars as shown in Fig. 5, where we notice a bimodal distributions of magnetic-field and spin-period of recycled pulsars (initial distributions of B and P at right parts of plots compared to the final evolved values at the left parts of plots). As compared to the observational distributions of binary pulsars, we notice that the both histograms for the MSPs (left parts of Fig. 5), theoretical and observed data, are very similar. For the spin period, more theoretical data than the observed values occurs at the regimes close to millisecond, which may imply that more MSPs may not evolve to their minimum spin period of about millisecond.

3.3. Spin-period Versus Accretion Mass ($P - \Delta M$)

To investigate the spin-period evolution with accretion mass, we consider the influences by initial conditions and accretion rate and plot the evolutionary curves in $P - \Delta M$ diagrams (see Fig. 6). As a detailed illustration, Fig. 6 implies the following results. (1). After accreting certain mass (e.g. $\sim 0.01 M_\odot$), the spin-period evolution seems independent of the initial magnetic-field. (2). The influence on $P - \Delta M$ by the initial spin-period on the spin evolution exists when $\Delta M < \sim 0.001 M_\odot$ and disappears when the accreted mass $\Delta M > 0.001 M_\odot$. When a small amount of mass ($\sim < 0.001 M_\odot$) is transferred, the spin-period mildly changes (Fig. 6), which may yield a HMXB with the spin-period of some seconds, such as Her X-1 (van der Meer et al. 2007) and Vela X-1 (Quaintrell et al. 2003). After a conveniently long time, with the weight of material accreted

$\sim 0.01 M_\odot$, NS is spun-up to a shorter period ($P \sim < 100ms$) which corresponds to the system of DNS, e.g. PSR 1913+16 (Breton 2009). The binaries with longer accretion phase, e.g. LMXBs, will accrete sufficient mass ($\Delta M \sim > 0.1 M_\odot$) from their companions and yield a lower magnetic-field and shorter spin-period ($P \sim < 20 ms$), as in the case of MSPs, e.g. SAX J 1808.4-3658 (Wijnands & van der Klis 1998; Wijnands 2005) and PSR J 1748-2446 (Lorimer, 2008). (3). At the beginning of accretion, NSs with different accretion rates follow different curves in the $P - \Delta M$ plane. After accreting $\sim 0.01 M_\odot$, the spin-period approximately follow the same track with different accretion rate, until to the same minimum period. Therefore, NSs in LMXBs, for the Z source with Eddington luminosity and Atoll source with less luminosity, e.g. $\sim 1\%$ Eddington accretion rate (Hasinger & van der Klis 1989), should have the similar spin frequencies while accreting $\sim 0.2 M_\odot$.

4. Summary and Discussion

Considering the influences exerted by the different initial magnetic-field, initial spin-period and the accretion rate, we investigate the evolutionary tracks of recycled pulsar in $B - P$ diagram. The main results are listed below.

(1). From the evolutionary tracks in $B - P$ diagram, we find that the magnetic-field of NS decays with accreting material, and the spin-up evolution proceeds at the same time. The primary effect of the fastness parameter is to force the evolutionary curves to reside below the equilibrium period line. The critical fastness (ω_c) can infer the final spin-period of recycled NS (maximum spin frequency), for instance, $\omega_c = 0.5$ will correspond to a spin of 650 Hz (1.54 ms), which is near the highest observed value of MSP and AMXP.

(2). The influences of the initial magnetic-field, spin-period and accretion rate are tested, respectively. The evolutionary curves present that the spin-period (frequency) decreases (increases) with the accretion and the minimum spin-period is insensitive to these two initial conditions when it is spun-up to $P \sim 10 ms$ ($\nu \sim 100 Hz$) after NS accreting about $\sim > 0.2 M_\odot$.

(3). It is found from the B-P diagram, a few observed MSPs locate above the "spin-up line", while the trajectories based on our model always lie below this line. Firstly, owing to the Ohmic dissipation, the buried field of MSP may re-emerge after accretion, which can account for a slightly increase of field of the star (e.g. Young & Chanmugam 1995; Bhattacharya 2008). Secondly, the magnetic model we use here is based on the "dilution of polar magnetic flux" due to accretion, which is idealized. Due to numerous plasma instabilities, the Rayleigh-Taylor instability at the disk-magnetosphere interface because of the high-density disc matter being supported against by the low-density magnetosphere plasma and Kelvin-Helmholtz instability because of the discontinuity in the angular velocity of matter at the boundary (Ghosh & Lamb 1979a), these instabilities may result in the penetration of the magnetosphere, prying the field lines aside and azimuthally wrapping the field lines by the disc matter (e.g. Romanova 2008; Kulkarni & Romanova et al. 2008), which may modify the field strength evolution then perturb the spin evolution.

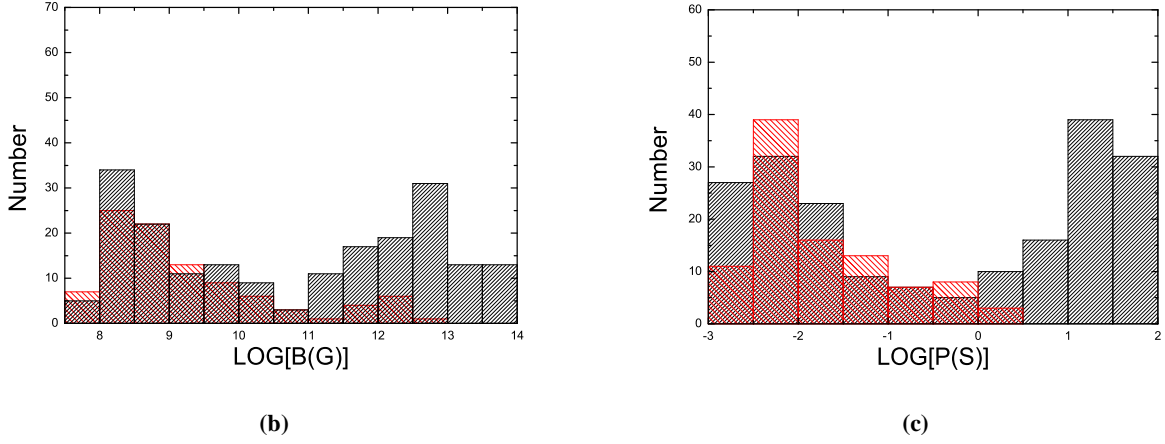


Fig. 5. Plots of histograms for spin-period and magnetic-field obtained from the calculation for the theoretical model and for the observed binary pulsars (red-shaded). In theoretical calculations, we assume that the initial B-field follows a Gaussian distribution, centered at 5×10^{12} G, and ranged from 5×10^{10} G (e.g. Hartman et al. 1997) to 10^{14} G (e.g. Kaspi 2010); As for the initial spin period, it is assumed to be Gaussian distribution, centered at 30 s, ranged from 0.5 s to 100 s; The different accretion rates are set from \dot{M}_{16} to \dot{M}_{18} . The theoretically evolved B-field and spin period values occurred at the left parts of plots, which are similar to the observed distributions.

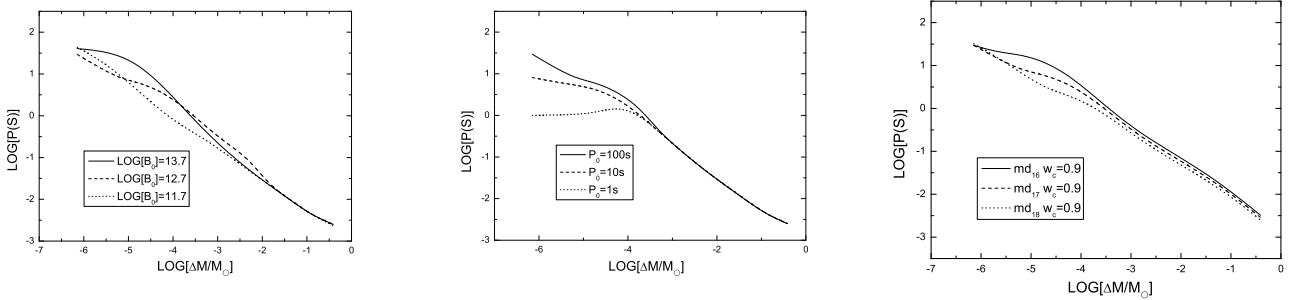


Fig. 6. Plots of spin-period versus accretion mass with different conditions, i.e., initial magnetic-fields (left), initial spin-periods (middle) and accretion rates (right), where the critical fastness parameter is set to be $\omega_c = 0.9$ in calculation. It is noticed that the initial conditions (B_0 and P_0) and accretion rate has little influence on the $P - \Delta M$ plot after the system accretes $\sim > 0.01 M_\odot$; In other words, the spin periods of NS/LMXBs should be primarily related to how much mass accreted.

(4). The formation of the fastest spin frequency of MSP is an interesting topic (Lorimer 2008; Chakrabarty et al. 2003; Chakrabarty 2005). The known fastest radio pulsar is PSR J1748-2446ad (Ter 5) at 716 Hz (Hessels et al. 2006), whereas the highest AMXP spin frequency in LMXBs is 619 Hz (e.g. Wijnands 2005). However, the recent report of 1122 Hz burst oscillation frequency, interpreted as a spin frequency, in XTE J 1739-285 (Kaaret et al. 2007) has been reported but not yet confirmed on account of the statistical significance (actual significance is only 3σ). Now the detected spin is less than the believed breaking spin frequency of pulsar of about ~ 1000 Hz (Lattimer & Prakash 2004), then what causes the special maximum spin frequency of MSP?

The spin evolution is affected by the accretion torque, which consists of two parts (Ghosh 1995; Frank et al. 2002): the stresses associated with matter accreting from the inner

edge of the disk ($N_0 \equiv \dot{M}(GMR_M)^{\frac{1}{2}}$) and that associated with the magnetic field coupling the star with the disk. The total torque N can be conveniently expressed in terms of N_0 and the dimensionless torque. The spin-down torques which balances the spin-up torque will also contribute to forming the maximum spin frequency. Slow rotators ($\omega_s < \omega_c$) are spun up ($n > 0$) by this accretion torque. $\omega_s < 1$ is presumed, since for $\omega_s > 1$ the steady accretion is of course impossible. Here, ω_c of approximately $\sim 0.3 - 0.5$ is the critical fastness at which the torque changes direction, thus the maximum spin frequency $\nu_s = 2\pi\Omega_s = \omega_c \nu_k \sim (0.3 - 0.5)\nu_k$, where $\nu_k = 2\pi\Omega_k$. The observed maximum upper kHz QPO frequency is 1330 Hz (van der Klis 2000; Zhang et al. 2006) that is interpreted as the Keplerian frequency ν_K of inner disk orbit, so this implies a maximum spin frequency to be about $\sim 400 - 665$ Hz which is consistent with observations. To limit the occurrence

of high spin of MSP over 1000 Hz, the braking torques have been considered. Electromagnetic braking torque can brake the stellar spin (Ghosh 1995, 2006), which are usually expressed in the form $n \propto \mu^2(\Omega_s/c)^3$, where μ is the magnetic dipole moment of the star. In NS/LMXB, the mass quadrupole can occur on account of the accretion that arises the gravitational wave (GW) radiation (Bildsten 1998; Melatos 2007; Melatos & Payne 2005; Melatos & Peralta 2010; Ghosh 2006; Vigelius, Payne & Melatos 2008; Watts et al. 2009). The angular momentum is lost from the emission of GW which may spin-down the NS. With accretion, the gravitational wave and accretion torques balance, but the total torque is effectively negative because the gravitational wave torque increases with accreting. Hence, there might arise a maximum spin frequency of several hundred Hertz for a MSP.

5. acknowledgements

We are grateful for the discussions with G. Hasinger, M. Mendez, and T. Belloni. This work is supported by the National Natural Science Foundation of China (NSFC 10773017) and the National Basic Research Program of China (2009CB824800).

References

- Archibald A. M., Stairs I. H. & Ransom S. M. et al. 2009, *Science*, 324, 1411
- Alpar M. A., Cheng A. F. & Ruderman M. A. et al. 1982, *Nature*, 300, 728
- Bhattacharya D. & van den Heuvel E. P. J. 1991, *Phys. Rep.*, 203, 1
- Bhattacharya D. & Srinivasan G. 1995, in *X-ray Binaries*, eds. Lewin W. H. G., van Paradijs J. and van den Heuvel E. P. J., (Cambridge University Press)
- Bhattacharya D. 2008, to appear in *Proceedings of "A Decade of Accreting Millisecond X-ray Pulsars"*, eds. R. Wijnands et al.
- Bildsten L. 1998, *ApJ.*, 501, L89
- Breton R. P. 2009, PhD thesis, arXiv:0907.2623
- Burderi L., D'Antona F., Menna M. T., di Salvo T., Robba N. 2002a, *Mem. Soc. Astron. Ital.*, 73, 1072
- Burderi L., D'Antona F. & Burgay M. 2002b, *ApJ.*, 574, 325
- Camilo F., Thorsett S. E. & Kulkarni S. R. 1994, *ApJ.*, 421, L15
- Chakrabarty D., Morgan E. H., Munro M. P. et al. 2003, *Nature*, 424, 42
- Chakrabarty D. 2005, *ASP Conf. Ser.*, 328, 279
- Cheng K. S. & Zhang, C. M. 1998, *A&A*, 337, 441
- Cheng K. S. & Zhang, C. M. 2000, *A&A*, 361, 1001
- Cumming A., Zweibel E. G. & Bildsten L. 2001, *ApJ.*, 557, 958
- Cumming A. 2005, *ASP Conf. Ser.*, 328, 311
- Ferrario L. & Wickramasinghe D. T. 2007a, *AIP Conference*, 968, 188
- Ferrario L. & Wickramasinghe D. T. 2007b, *AIP Conference*, 968, 194
- Elsner R. F., & Lamb F. K. 1977, *ApJ.*, 215, 897
- Francischelli G. J., Wijers R. A. M. J. & Brown G. E. 2002, *ApJ.*, 565, 471
- Frank J., King, A. & Raine D. J. 2002, *Accretion Power in Astrophysics*, Cambridge, UK
- Geppert U. & Urpin V. 1994, *MNRAS*, 271, 490
- Geppert U., Page D. & Zannias T. 1999, *A&A*, 345, 847
- Ghosh P. & Lamb F.K. 1977, *ApJ.*, 217, 578
- Ghosh P. & Lamb F.K. 1979a, *ApJ.*, 232, 259
- Ghosh P. & Lamb F.K. 1979b, *ApJ.*, 234, 296
- Ghosh, P. & Lamb, F. K. 1992, in *X-ray Binaries and Recycled Pulsars*, ed. E. P. J. van den Heuvel, S. A. Rappaport (Dordrecht: Kluwer), 487
- Ghosh P. 1995, *JApA*, 16, 289
- Ghosh P. 2006, *Rotation and Accretion Powered Pulsars*, World Scientific, India
- Hartman J.W. et al. 1997, 325, 1031
- Hasinger G. & van der Klis M. 1989, *A&A*, 225, 79
- Halpern, J. P. & Gotthelf, E. F. 2010, *ApJ.*, 709, 436
- Hessels J. W., Ransom S. M. & Stairs I. H. et al. 2006, *Science*, 311, 1901
- Hurley J. R., Tout C. A., Wickramasinghe D. T., Ferrario, L. & Kiel P. D. 2009, *MNRAS*, 402, 1437
- Hobbs G. & Manchester R. 2004, *ATNF Pulsar Catalogue*, http://www.atnf.csiro.au/research/pulsar/psrcat/psrcat_help.html
- Inogamov N. A. & Sunyaev R. A., 1999, *AstL.*, 25, 269
- Kaaret P., Prieskorn Z. & in't Zand J. et al. 2007, *ApJ.*, 657, L97
- Kaspi V. M. 2010, *PNAS*, 107, 7147, arXiv:1005.0876v1
- Konar S. & Bhattacharya D. 1999, *MNRAS*, 303, 588; 308, 795
- Konar S., & Choudhury A. 2004, *MNRAS*, 348, 661
- Kouveliotou C. 2003, *AAS*, 203, 7501
- Kulkarni A. K., & Romanova M. M. 2008, *MNRAS*, 386, 673
- Lamb F. K. & Yu W. 2005, in *Spin rates and magnetic fields of millisecond pulsars*, in *Binary Radio Pulsars*, ed. F. A. Rasio & Stairs I. H. (ASP Conference Series, Vol. 328), 299
- Lattimer J. M. & Prakash M. 2004, *Science*, 304, 536
- Li X. D., Wang Z. R., 1996, *A&A*, 307, L5
- Li X. D. & Wang Z. R. 1999, *ApJ.*, 513, 845
- Lorimer D. R. 2008, *Living Rev. Relativity*, 11, 8 <http://relativity.livingreviews.org/Articles/lrr-2008-8/>
- Lovelace R. V., Romanova M. M. & Bisnovatyi-Kogan G.S. 2005, *ApJ.*, 625, 957
- Lyne A. G., Burgay M., Kramer M. et al. 2004, *Science*, 303, 1153
- Manchester R. N., Hobbs G. B., Teoh A. & Hobbs M. 2005, *AJ*, 129, 1993
- Melatos A. 2007, *AdSpR*, 40, 1472
- Melatos A. & Phinney E. S. 2001, *PASA*, 18, 421
- Melatos A. & Payne D. 2005, *ApJ.*, 623, 1044
- Melatos A. & Peralta C. 2010, *ApJ.*, 709, 77
- Payne D. & Melatos A. 2004, *MNRAS*, 351, 569
- Quaintrell H., Norton A. J. & Ash T. D. C. et al. 2003, *A&A*, 401, 313
- Radhakrishnan V. & Srinivasan G. 1982, *Curr. Science*, 51, 1096
- Romani G. M., 1990, *Nature*, 347, 741

- Romanova M. M., Kulkarni A. K. & Lovelace R. V. E. 2008, *ApJ.*, 673, L171
- Shapiro S. L. & Teukolsky S. A. 1983, *Black Holes, White Dwarfs and Neutron Stars*. Wiley, New York
- Shibazaki N., Murakami T., Shaham J. & Nomoto K. 1989, *Nature*, 342, 656
- Taam R. E. & van den Heuvel E. P. J. 1986, *ApJ.*, 305, 235
- Urpin V. & Geppert U. 1995, *MNRAS*, 275, 1117
- Urpin V. & Konenkov D. 1997, 284, 741
- Urpin V., Geppert U. & Konenkov D. 1997, *MNRAS*, 295, 907
- Urpin V., Geppert U. & Konenkov D. 1998, *A&A*, 331, 244
- van den Heuvel E. P. J. 1995, *JA&A*, 16, 255
- van den Heuvel E. P. J. & Bitzaraki O. 1994, *MmSAI*, 65, 237
- van den Heuvel E. P. J. & Bitzaraki O. 1995a, *A&A*, 297, L41
- van den Heuvel E. P. J. & Bitzaraki O. 1995b, In: *The Lives of the Neutron Stars*, Kluwer Academic Publishers, Dordrecht
- van den Heuvel E. P. J., 2004, *science*, 303, 1143
- van der Klis M. 2000, *ARA&A*, 38, 717
- van der Meer A., Kaper L., van Kerkwijk M. H., Heemskerk M. H. M. & van den Heuvel E. P. J. 2007, *A&A*, 473, 523
- Vigelius M., Payne D., Melatos A. 2008, *Proceedings of the 11th Marcel Grossmann Meeting on General Relativity*, World Scientific, arxiv: 0811.2031
- Watts A.L. et al. 2009, *MNRAS*, 389, 839
- Wickramasinghe D. T., Hurley J. R., Ferrario L., Tout C. A. & Kiel P. D. 2009, *JPhCS.*, 172, 2037
- Wijnands R. & van der Klis M. 1998, *Nature*, 394, 344
- Wijnands, R. 2006, *Trends in Pulsar Research*, ed. J. A. Lowry (New York, USA: Science Publishers, Inc.), 53
- Wijers R. A. M. J. 1997, *MNRAS*, 287, 607
- Yin H.X., Zhang C.M. & Zhao Y.H. 2007, *A&A*, 471, 381, arXiv:0705.1431
- Young E.J. & Chanmugam G. 1995, *ApJ*, 442, L53
- Zhang C. M. & Kojima Y. 2006, *MNRAS*, 366, 137
- Zhang C. M., Yin H. X., & Zhao Y. H., et al. 2006, *MNRAS*, 366, 1373.

